RESEARCH ARTICLE

Stress field change around the Mount Fuji volcano magma system caused by the Tohoku megathrust earthquake, Japan

**Eisuke Fujita · Tomofumi Kozono · Hideki Ueda ·
Yuhki Kohno · Shoichi Yoshioka · Norio Toda ·
Aiko Kikuchi · Yoshiaki Ida**

Abstract Crustal deformation by the M_w 9.0 megathrust Tohoku earthquake causes the extension over a wide region of the Japanese mainland. In addition, a triggered M_w 5.9 East Shizuoka earthquake on March 15 occurred beneath the south flank, just above the magma system of Mount Fuji. To access whether these earthquakes might trigger the eruption, we calculated the stress and pressure changes below Mount Fuji. Among the three plausible mechanisms of earthquake–volcano interactions, we calculate the static stress change around volcano using finite element method, based on the seismic fault models of Tohoku and East Shizuoka earthquakes. Both Japanese mainland and Mount Fuji region are modeled by seismic tomography result, and the topographic effect is also included. The differential stress given to Mount Fuji magma reservoir, which is assumed to be located to be in the hypocentral area of deep long period earthquakes at the depth of 15 km, is estimated to be the order of about 0.001–0.01 and 0.1–1 MPa at the boundary region between magma reservoir and surrounding medium. This pressure change is about 0.2 % of the lithostatic pressure (367.5 MPa at 15 km depth), but is enough to trigger an eruptions in case the magma is ready to erupt. For Mount Fuji, there is no

evidence so far that these earthquakes and crustal deformations did reactivate the volcano, considering the seismicity of deep long period earthquakes.

Introduction

The relationship between large earthquakes and eruptions has been widely discussed. In 1835, the Minchinmavida and Cerro Yanteles volcanoes in Chile erupted within 1 day after an M_w 8.1 earthquake (Manga and Broadsky 2006). Cordon Caulle volcano, located 240 km from the megathrust Chile earthquake (M_w 9.5) in 1960, began to erupt 38 h after; this was its first eruption in 16 years (Lara et al. 2004). Three other volcanoes erupted during the following 3 years, one as far away as 500 km. After the Kamchatka earthquake (M_w 9.0) in 1952, six volcanoes erupted in three successive years, some for the first time in history. Similarly, Karymsky Volcano and Akademia Nauk Volcano also erupted just 2 days after the 1996 Kamchatka peninsula earthquake about 10–20 km to the south (Walter 2007). In 1992, a huge eruption of Pinatubo in the Philippines occurred 11 months after the M_w 7.8 Luzon earthquake 100 km away (Bautisa et al. 1996). Recent Sumatra earthquakes in 2004 (M_w 9.3) and 2005 (M_w 8.7) also disturbed the volcanic chains around Sumatra and the Andaman region (Walter and Amelung 2007). No significant volcanic activity occurred for a few days after the M_w 9.3 earthquake, except for a mud volcano in the Andaman Islands (Mellors et al. 2007). However, the second major earthquake (M_w 8.7) on March 28 triggered an eruption of the Talang volcano, Krakatoa, within 12 days (Walter and Amelung 2007). Two days after the M_w 6.7

E. Fujita (✉) · T. Kozono · H. Ueda · Y. Kohno
National Research Institute for Earth Science and Disaster
Prevention, Tennodai 3-1,
Tsukuba, Ibaraki 305-0006, Japan
e-mail: fujita@bosai.go.jp

S. Yoshioka
Department of Earth and Planetary Sciences, Faculty of Science,
Kobe University, 1-1 Rokkodai-cho, Nada,
Kobe 657-8501, Japan

N. Toda · A. Kikuchi · Y. Ida
Advance Soft Corporation, Akasaka 1-9-20, Minato,
Tokyo 107-0052, Japan

aftershock on April 12, 2005, certain abnormal activities of the Talang and Tangkubuanparahu volcanoes were detected and small eruptions were observed (Walter and Amelung 2007). Barren Island, India, began to erupt 5 months after the main shock (Walter and Amelung 2007). Also, submarine volcanoes in the Nicobar Islands became active 1 month after the main shock (Walter and Amelung 2007).

The last eruption of Mount Fuji, Japan, in 1707, was also considered to have relation with a major thrust earthquake in this area (Koyama 2002, 2007). In 1704, 3 years before the 1707 eruption, seismic swarms were observed 35 days after the Genroku Kanto earthquake (M_w 8.1) occurred 100 km to the east, but no eruption occurred. Historical records indicate local seismic swarms around Mount Fuji and the Hoei Tokai-Nankai earthquake (M_w 8.6) in September 1707, occurring 200 km to the southwest on October 28. Beginning on December 3, seismic swarms were observed several times per day and dozens of earthquakes were felt from December 15; Mount Fuji then began to erupt, and earthquakes were also associated with the eruption from December 16.

Some conceptual models relating earthquakes and volcanic eruption have been proposed. If the stress and strain around the volcanic system increases due to an earthquake, magma is squeezed and goes up through the fractures, and this may lead to an eruption (e.g., Nakamura 1977; Nostro et al. 1998). However, a decrease in stress and strain field around the magma system can also disturb the magma activity. When the pressure in the magma is reduced, bubble formation is promoted. The expansion of a magma chamber may rupture the surrounding rock and make cracks, through which magma can migrate upward (e.g., Marzocchi et al. 1993; Hill et al. 1993; Linde et al. 1994). In addition, the expanding stress field around the magma system also promotes to create more paths for magma, allowing it to rise more easily than before. Stress changes caused by large earthquakes can be categorized into three models (Hill et al. 2002): static stress change, quasistatic stress change, and dynamic stress change. Static stress change can be evaluated as the difference between the pre-earthquake and post-earthquake stress fields. This stress change is produced by the dislocation of a seismic fault but is effective only in the region close to the fault, since the magnitude of stress change attenuates by $1/r^3$, where r is the distance from the earthquake fault. Quasistatic stress change is caused by the viscoelastic relaxation of the lower crusts and the upper mantle around the earthquake fault. The lag time preceding an eruption due to static and quasistatic mechanisms is on the order of months to years. Dynamic stress change is related to seismic waves, which attenuate by $1/r^{1.6}$, or to surface seismic waves, which attenuate by $1/r^2$. The lag time is minutes to hours. Seismic waves can create new bubbles by pressure perturbation to excite volcanic eruption (e.g., Walter et al. 2009). The critical excess pressure to create
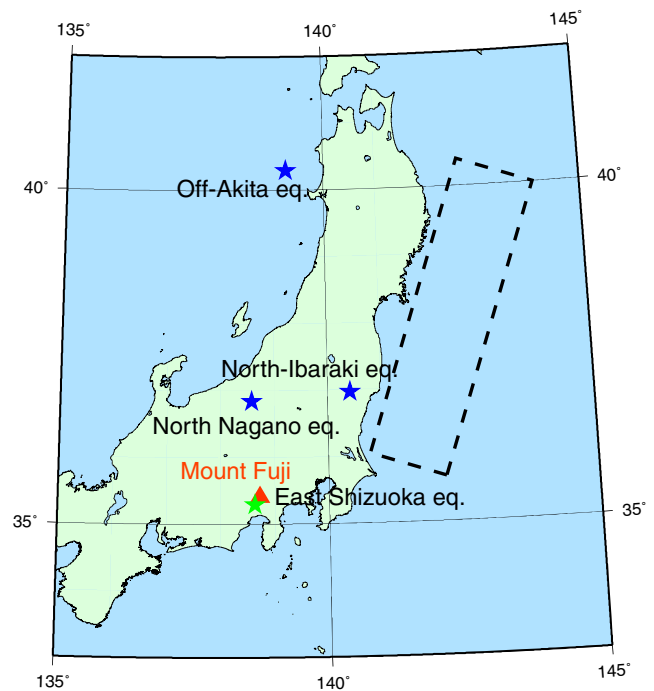

Fig. 1 Epicenters of earthquakes triggered by the Tohoku megathrust earthquake. The fault region of the Tohoku megathrust earthquake is 500×200 km, and Mount Fuji is located 200 km to the southwest. The M_w 5.9 East Shizuoka earthquake occurred on March 15, 2011, 4 days after the Tohoku megathrust earthquake

new seeds of bubbles is estimated to exceed 100 MPa for homogeneous creation and a few 1 MPa for heterogeneous creation (Navon and Lyakhovsky 1998). This mechanism also depends highly on the state of the magma. Sumita and Manga (2008) studied the rheological characteristics of suspensions subject to seismic wave perturbation and the possibility of volcanic eruptions being triggered. From another

Table 1 Fault parameters of the Tohoku and East Shizuoka earthquakes. Parameters for the Tohoku earthquake are from Ozawa et al. (2011). Those for the East Shizuoka earthquake were obtained by inversions from GPS and tiltmeter data from the GEONET and NIED networks, applying the method of Ueda et al. (2005)

| Parameters	Tohoku 1	Tohoku 2	East Shizuoka
Latitude	38.80 N	37.33 N	35.3161 N
Longitude	144.00 E	142.80 E	138.7130 E
Depth (top), km	5.1	17	7
Length, km	186	194	6
Width, km	129	88	8
Strike, degrees	203	203	24
Dip, degrees	16	15	80
Rake, degrees	101	83	20
Dislocation, m	24.7	6.1	0.86
Magnitude	8.8	8.3	6.0

point of view, Linde and Sacks (1998) and Manga and Broadsky (2006) present a statistical evaluation of the relation between earthquakes and volcanic eruptions.

Characteristics of Tohoku megathrust and East Shizuoka earthquakes

On March 11, 2011, the Tohoku megathrust earthquake M_w 9.0 (also called the Off the Pacific Coast of Tohoku earthquake) in Japan ruptured an area as large as 500×200 km^2 along the subduction zone of the Pacific plate (Asano et al.

2011) and disturbed the tectonic field of a wide area of the eastern Japanese mainland (Fig. 1). In addition, ground deformation caused by the Tohoku earthquake triggered numerous aftershocks and triggered earthquakes (e.g., the North Nagano earthquake (M_w 6.3), the off-Akita earthquake (M_w 6.2) on March 12, and the North Ibaraki earthquake (M_w 5.8) on March 19; Toda et al. 2011). The seismicity at about 20 volcanoes in Japan increased shortly after this megathrust earthquake, but no eruptions occurred (Japan Meteorological Agency 2011). Mount Fuji also exhibited the increase of local volcano–tectonic earthquakes and a triggered earthquake occurred, the East Shizuoka earthquake M_w 5.9 on

Fig. 2 Seismicity around Mount Fuji in 2010 and 2011. *Red circles* hypocenters of DLP events, *blue circles* tectonic earthquakes. The East Shizuoka earthquake (March 15, 2011) occurred on the south flank of Mount Fuji at a depth of 12 km. DLP activity was spasmodic and did not change significantly even after the East Shizuoka earthquake. Remote aftershocks were recorded in the AS region (*dashed circle*)
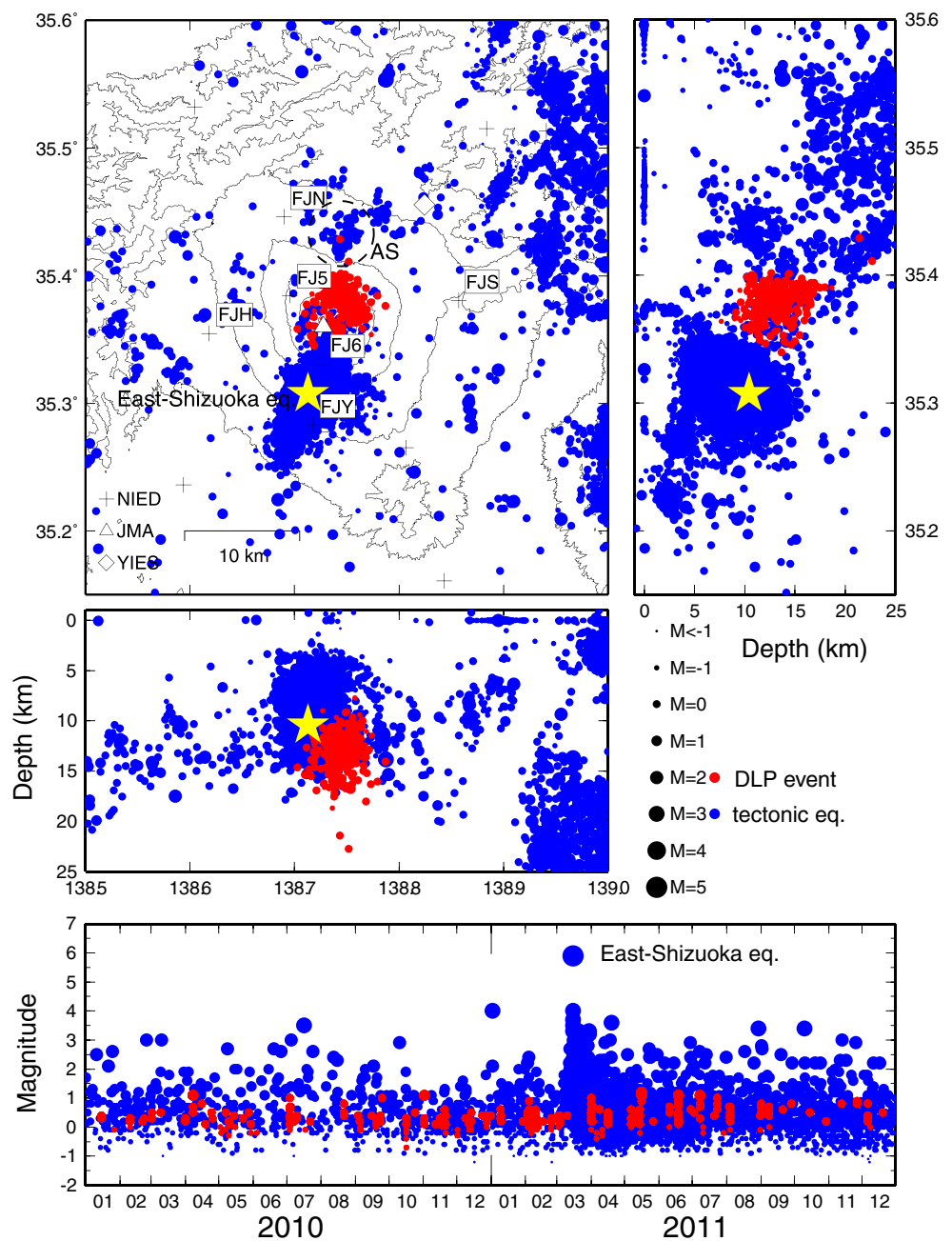
March 15, 4 days after the Tohoku megathrust earthquake, beneath the south flank of Mount Fuji, located 300 km southwest of the southern edge of the megathrust fault. This earthquake was caused by brittle failure inside the Eurasian plate, where many tectonic (i.e., not volcanic) earthquakes (less than M_w 2) had been observed. The hypocenter of this earthquake is very close to the magmatic system of Mount Fuji, so it is feared that Mount Fuji may start to erupt. But there have been no clear such signals suggesting the triggering of volcanic activity on Mount Fuji as increasing deep long-period earthquakes and crustal deformations 1 year after the earthquake.

Mount Fuji is located above a complex area where the Pacific and Philippine Sea Plates (PHS) subduct beneath the Eurasian plate. Many reports discuss the distribution of the three plates' boundaries; however, the detailed structure of the plates and the magma system around Mount Fuji is still unclear (e.g., Nishimura et al. 2007). Historical eruptive craters are aligned NW–SE passing the summit, due to the maximum principal tectonic stress in this direction (Nakamura 1977). No eruptions have occurred since 1707, but an abnormal increase in deep

long period (DLP) events occurred in 2000 and 2001, shortly after the 2000 Miyakejima volcano eruption and numerous crustal deformations around the Izu–Bonin volcanoes 100 km to the southeast (Ukawa 2005). After this seismic swarm, we recorded no specific seismic or geodetic activity up to 2011.

This study evaluates the disturbance of the Mount Fuji magma system caused by the Tohoku and East Shizuoka earthquakes, and discusses possible mechanisms leading to an eruption of Mount Fuji. Among the proposed mechanisms relating earthquakes and volcanic eruptions, we will focus on static stress changes in this paper as a first step, since our analysis will concentrate on mid-long-term effects and evaluate the possibility of volcanic eruption in future. Static–stress change can cause the change of magma condition and such a succeeding state changes like bubbling due to depressurization may occur with some time delays and this may be related the eruption. The complex rupture propagation occurring along the fault has also been considered recently by, e.g., Simons et al. (2011) and Koketsu et al. (2011), and we briefly consider this fault model in Appendix.
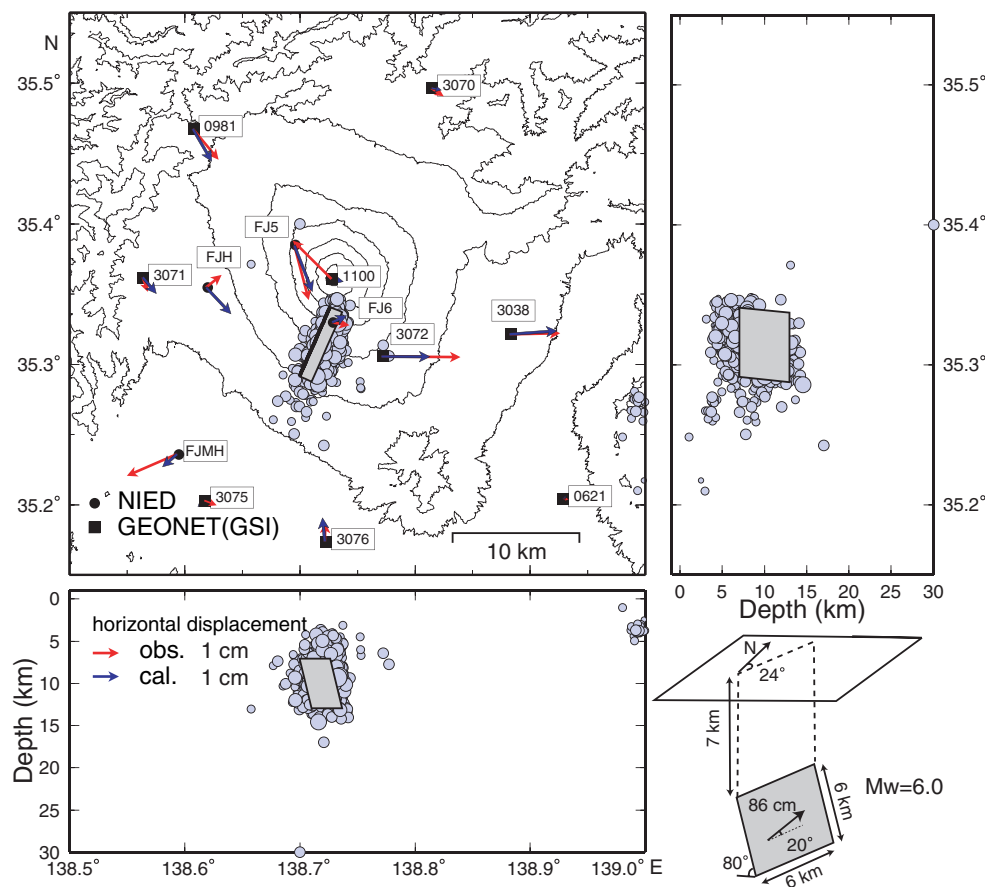

Fig. 3 Inversion result of the source fault of the East Shizuoka earthquake. We estimated the dislocation of an 86 cm fault source of 6× 6 km fault with a strike of N24E, depth of 7 km, dip of 80, and rake of 20 based on GPS data from NIED and GEONET (Graphical Survey Institute, Japan). *Red arrows* observation, *blue arrows* calculation displacements

In addition, our study has not yet considered the post-seismic crustal deformation (Marzocchi et al. 2003). This viscoelastic deformation in longer time scale would produce stress concentration around the boundary of crust and magma system and this may lead to an eruption.

Modeling procedures

We evaluate static crustal stress change due to earthquakes around a volcanic system in two steps. First, we identify the seismic fault parameters of the earthquakes by inverting the observation data. Second, we calculate the stress perturbations on a magmatic system using the finite element method.

Seismic fault parameters of Tohoku and East Shizuoka earthquakes

The fault parameters of the Tohoku megathrust earthquake were estimated by Ozawa et al. (2011) using the Japan-wide Global Positioning System (GPS) network, GEO-NET (Table 1). To evaluate stress changes around the Mount Fuji region by finite element method (FEM), we apply these fault parameters in the next section.

To determine source fault of the East Shizuoka earthquake, we performed an inversion analysis of the ground deformation data from GPS and tiltmeters using the generic algorithm method (Ueda et al. 2005). We determined the best-fit fault model to be almost strike-slip with some reverse components, located a few kilometers south of the summit trending from depths of 7–12 km (Figs. 2 and 3). The dislocation was 86 cm toward the NNE with a strike of 24°, dip of 80°, and rake of 20° (Table 1). Aftershocks of the East Shizuoka earthquake also occurred along this fault.

FEM modeling

We defined two areas to numerically simulate crustal deformation, i.e., the wide Japan area of 1,826 km EW×2,000 km NS and 400 km UD divided into 100×120×30 meshes, and the local Fuji area of 40 km EW×40 km NS×40 km UD area is divided into 56×56×50 meshes. The EW, NS, and bottom boundaries of the wide Japan area are replaced by "infinite elements" to remove the effect of reflection by boundaries (Han and Wu 1985; Wolf and Song 1996). The horizontal and bottom boundaries of the Fuji area are assigned to connect the calculated results for a wide area at each node. We also include the effect of topography and the seismic velocity structure discussed by Matsubara et al.

(2008). From the result of seismic tomography, we obtain Vp and Vs at each element. The density ρ can be estimated from Vp through the empirical equation by Birch (1961), derived from the laboratory experiments. The elastic moduli and Poisson ratios at each element can be also calculated by Vp, Vs, and ρ. Loading is calculated at the seismic-fault elements, but gravity is not considered. The quantitative effects of the topography and heterogeneity of the crust are given in the Appendix.
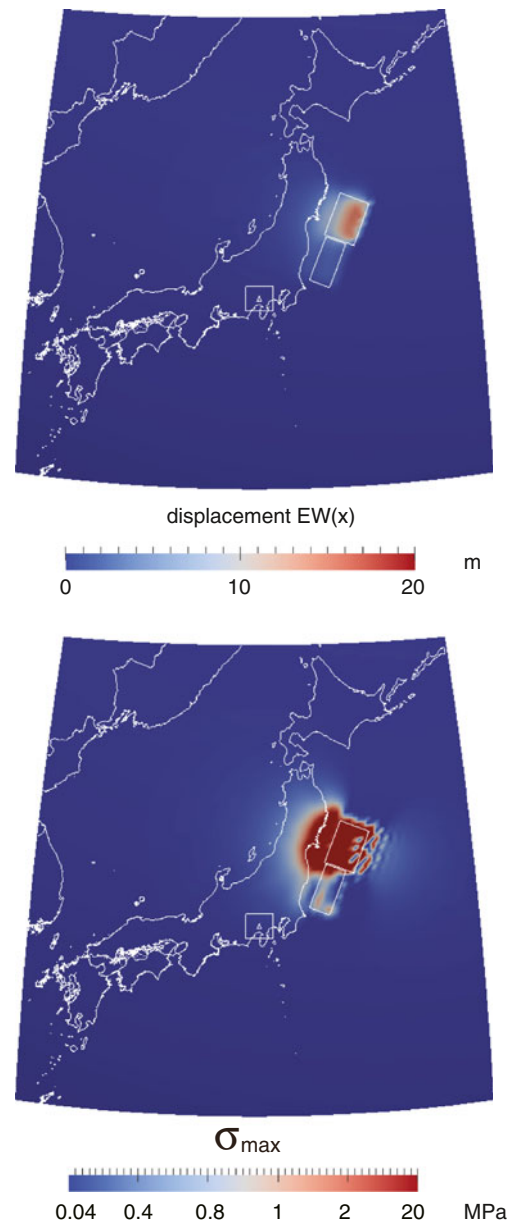

Fig. 4 Displacements EW(x) and maximum principal stress σ_{max} due to the Tohoku earthquake as calculated by the finite element method. The *lines* suggest the direction of maximum principal stress. The source fault parameters are based on the inversion result of Ozawa et al. (2011). The Mount Fuji region is indicated as a square in the central part of the figure. The unit for the displacement (stress) is meter (Mega Pascal)

Fig. 5 a Displacements of EW (x), NS(y), and UD(z) components around Mount Fuji as calculated by the finite element method for the Tohoku, East Shizuoka earthquakes, and for the sum of the two earthquakes. The seismic wave velocity structure around the Mount Fuji region is based on Nakamichi et al. (2007) and we assume a spherical magma reservoir whose center is 1.4 km NE of the summit at a depth of 15 km with a radius of 3,000 m, where the upper part of DLP event hypocenters region is located. In **b**, the maximum and minimum principal stresses and the differential stresses are depicted. The *lines* in the σ_{max} and σ_{min} distributions indicate their directions. Those in σ_{dif} indicate the σ_{max} directions. The unit for the displacement (stress) are meters (megapascal). In **c**, the average stress, equal to (σ_{max} + σ_{mid} + σ_{min})/3 and volumetric strain are depicted. The *dashed circles* indicate the region of magma reservoir
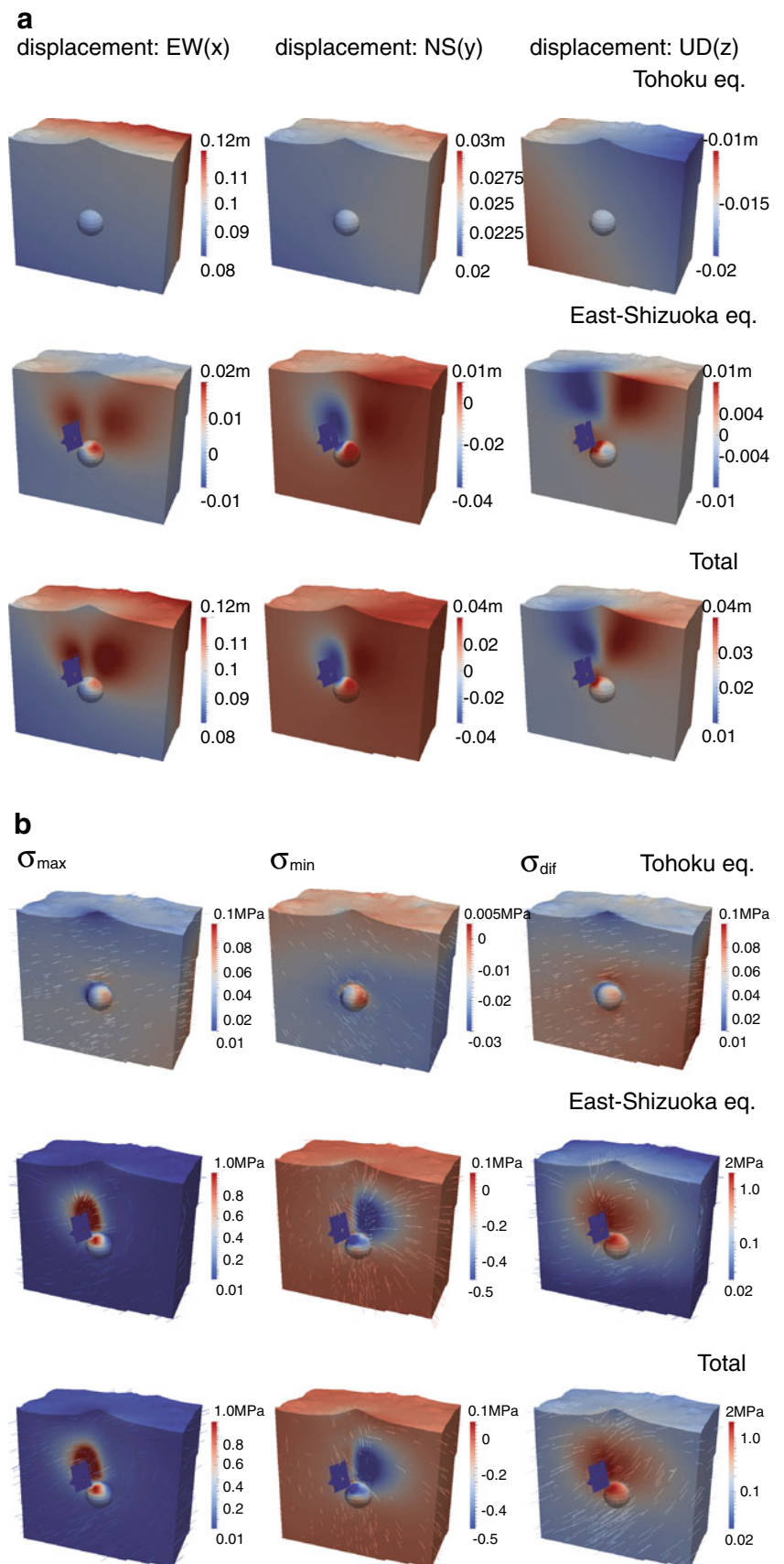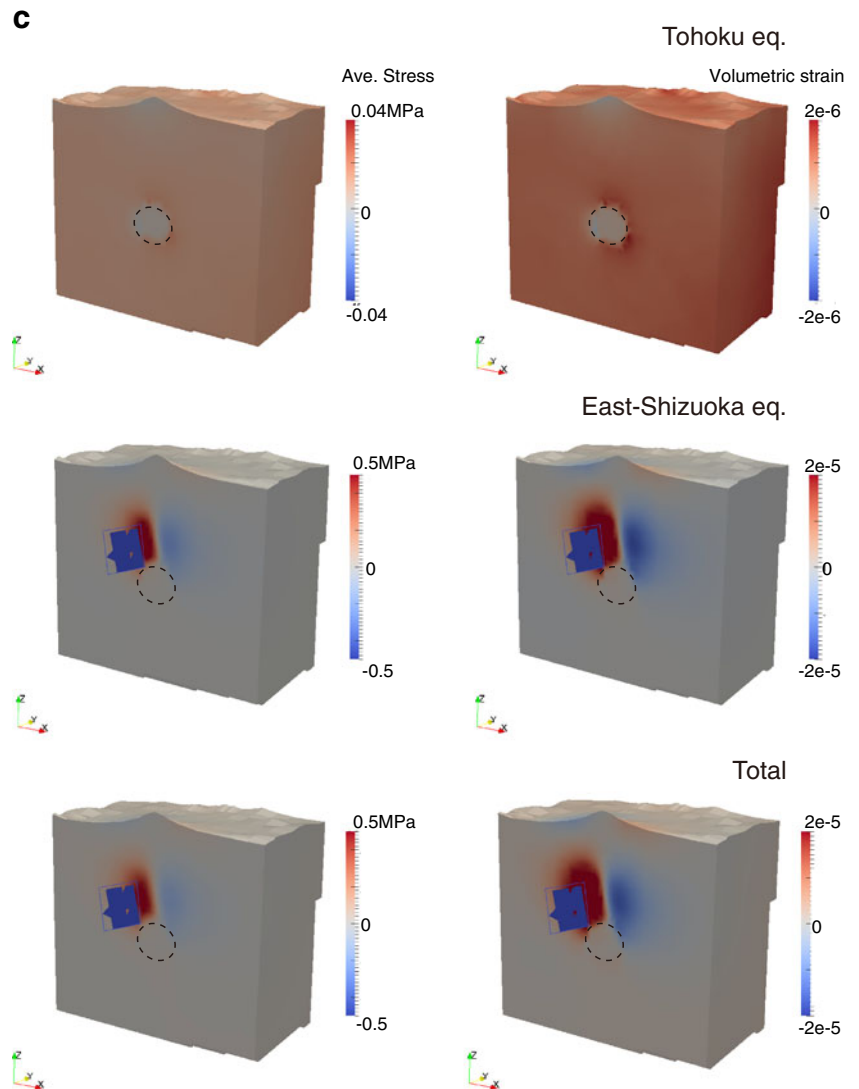
Fig. 5 (continued)

As for the magma properties in the subsurface volcanic plumbing system of Mount Fuji, Nakamichi et al. (2007) indicates a low Vp (P wave velocity), low Vs (S wave velocity), and low Vp/Vs anomaly at depths of 7–17 km; and a low Vp, low Vs, and high Vp/Vs anomaly at depths of 15–25 km. The former suggests the existence of supercritical volatile fluids (H_2O and CO_2) and the latter suggests the accumulation of basaltic melts. Based on these facts, we assume a simple spherical magma reservoir 1.4 km northeast of the summit of Mount Fuji, with a center depth of 15 km below sea level and a radius of 3,000 m, corresponding to the source region of DLP events. This is an assumption of the depth that gives the maximum effect to the magma reservoir and the sensitivity of the depth is discussed in Appendix. The Poisson's ratio in this magma region is estimated as 0.24 based on the inversion result of Vp/Vs=1.7 in the DLP area of Mount Fuji by Nakamichi et al. (2007). We applied these settings to calculate stress and displacement changes using FEM code, Advance/FrontSTR (Kikuchi and Dong 2011; Toda 2011), and visualized the numerical results using Paraview (www.paraview.org).

Results of numerical simulation

Figure 4 depicts the calculated EW displacement and maximum principal stress change due to the Tohoku earthquake over the entire Japanese mainland. These results are consistent with the observations and analysis of Ozawa et al. (2011). The Mount Fuji area is depicted as a square in the bottom part. Figure 5a presents the calculated distributions of displacements around Mount Fuji for the Tohoku, East Shizuoka earthquake, and the total displacements of two earthquakes. The displacement due to the Tohoku

Fig. 6 Displacement and maximum principal stress σ_{max} vectors inside the magma reservoir in response to Tohoku and East Shizuoka earthquakes. The *color* indicates the magnitude of σ_{max} and the length of the vector corresponds to the magnitude of displacement in the top plates
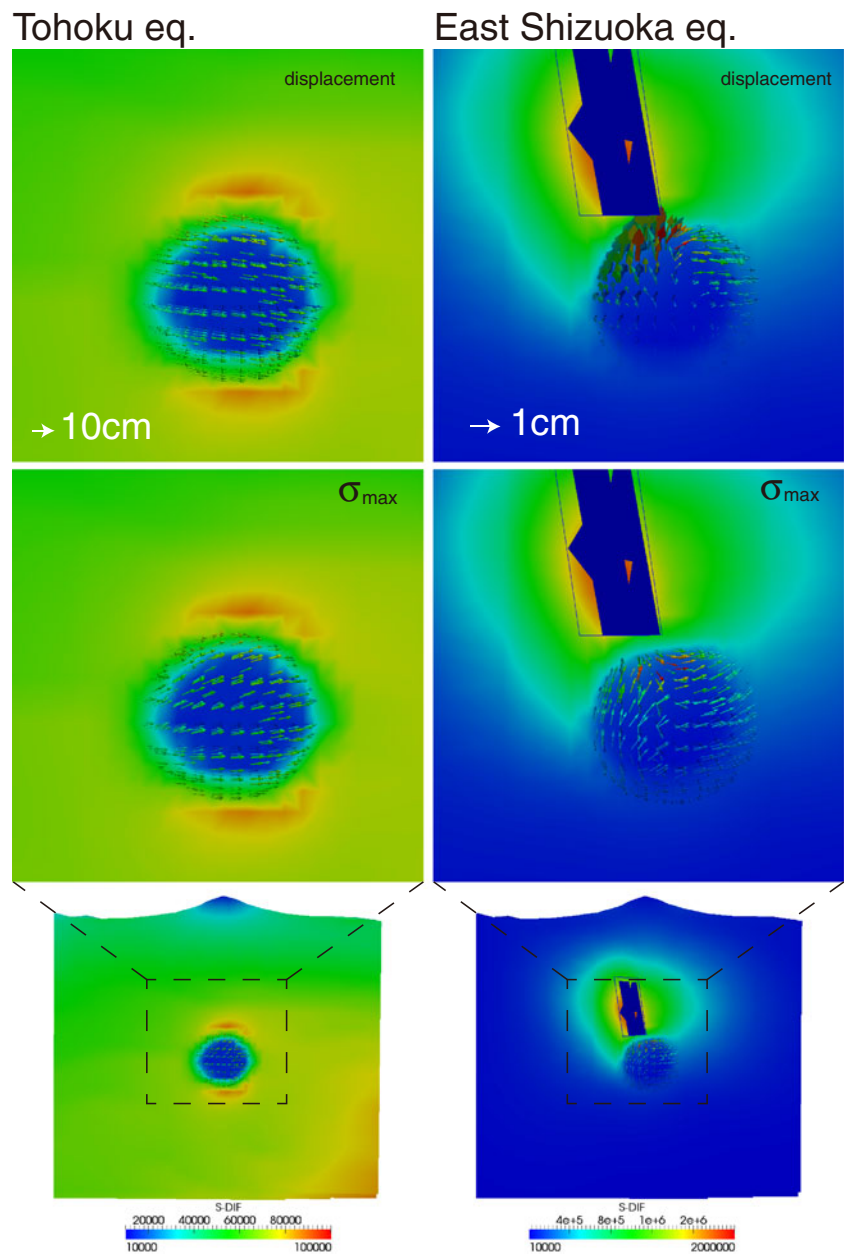
earthquake (Fig. 5a, top) is about 0.1 m EW(x), 0.02 m NS (y), and 0.01 m UD(z); the eastward movement is thus significant. For the East Shizuoka earthquake (Fig. 5a, middle), the fault is depicted as a square located just above a spherical reservoir. The EW(x) and NS(y) displacement patterns are coincident with the observation in Fig. 3. The UD(z) displacement suggests that the surface of the assumed spherical reservoir elevates more than 0.01 m in the western part and lowers less than 0.01 m in the eastern part. Figure 5a, bottom, indicates the sum of the displacements caused by the two earthquakes, but it is noted that we calculate only static stress change and do not consider temporal changes by post-seismic crustal deformation.

Figure 5b lists the maximum (σ_{max}), minimum (σ_{min}) principal stresses, and the differential stress (σ_{dif}) in the left, middle and right columns, respectively, for the Tohoku and East Shizuoka earthquakes as well as the total change. The distribution of the differential stress suggests where a fracture is likely to occur. For Tohoku earthquake, the axis of σ_{max} is in NE–SW direction and the significant σ_{dif} of the order of 0.1 MPa are identified at the top and bottom (a little bit east) boundary of the assumed spherical magma reservoir. For the East Shizuoka earthquake, the seismic fault is located to the southwest above the magma reservoir and the upper hemisphere feels the σ_{dif} as large as 1.6 MPa in maximum. This suggests that the fault movement of the

Fig. 7 Seismicity around Mount Fuji from 1996 to 2011. *Red circles* correspond to hypocenters of DLP events, and *blue circles* correspond to tectonic earthquakes. DLP activity increased in 2000 and 2001, shortly after the Miyakejima volcano eruption and huge ground deformation on Izu peninsula 100 km southeast of Mount Fuji
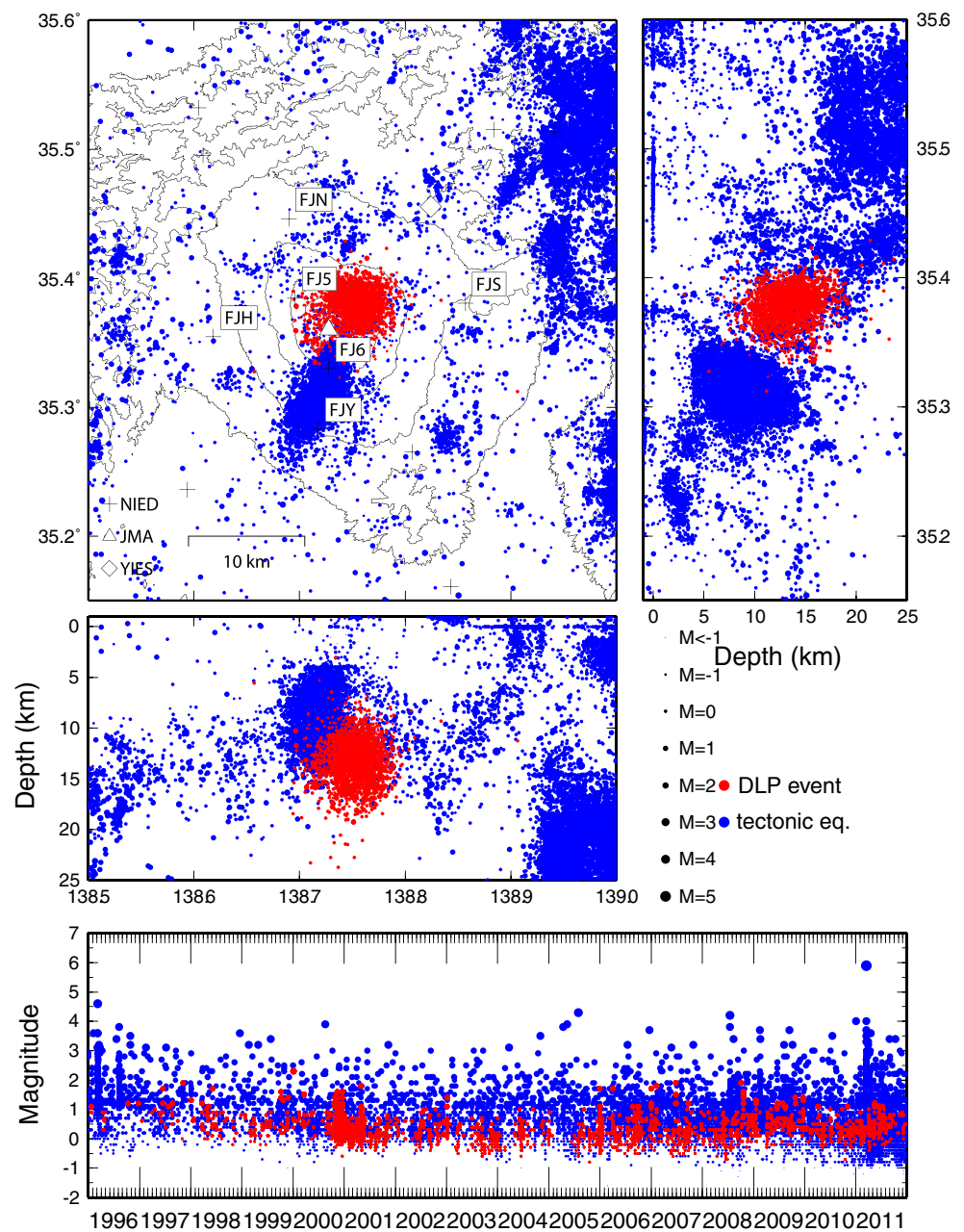
East Shizuoka earthquake pushed down the upper part of the magma reservoir. The total effect is mainly governed by the East Shizuoka earthquake. Figure 5c summarizes the average stress, equal to $(\sigma_{max} + \sigma_{mid} + \sigma_{min})/3$, and volumetric strain. The signs of positive average stress and volumetric strain correspond to the stress from inside to outside and expansive strain, respectively. The stress changes inside the magma reservoir are in the order of 0.01 MPa, which is also identified in Fig. 10 of Appendix, and the significant stress disturbance is concentrated at the boundary between magma reservoir and the surrounding medium.

In addition, we will evaluate the stress changes in magma reservoir. We assume a spherical magma reservoir with

Poisson's ratio of 0.24. In Fig. 6, we plot the vectors of displacement and σ_{max} changes inside the magma reservoir caused by Tohoku and East Shizuoka earthquakes. For Tohoku earthquake, all portions are almost uniformly pulled toward east. For East Shizuoka earthquake, the distributions of vectors are more complicated. The deformation is significant in the upper hemisphere, and the eastern hemisphere expands toward east and the western hemisphere moved upward. So the deformation and perturbation are not uniform and depend on the position in and surface of the magma reservoir. Total volume change of the magma reservoir is about 0.05 and -0.05 m^3 for Tohoku and East Shizuoka earthquake, respectively, almost negligible. However, the deformation within the
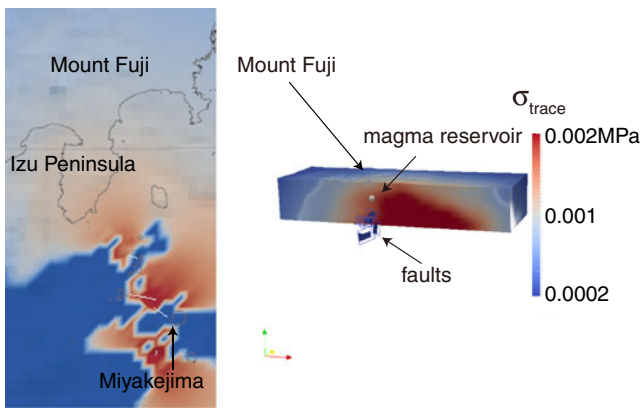
Fig. 8 Stress change due to the seismic swarm and ground deformation off the Izu peninsula in 2000. The source fault parameters are from Nishimura et al. (2001)

magma region is heterogeneous, and hence local volume changes might still play a role in triggering an eruption.

Discussion

We obtained stress changes of 0.001–1 MPa caused by the Tohoku and East Shizuoka earthquakes on the magma system beneath Mount Fuji, and these stress perturbations are concentrated at the boundaries between magma reservoir and surrounding elastic medium. Our interest is in whether these disturbances are sufficient to excite the magma and trigger an eruption. Here, we consider two kinds of processes leading to an eruption. The first process is the promotion of bubbling due to depressurization. Expansive crustal deformation reduces the magma pressure. This depressurization process promotes exsolving of volatile components like H_2O and CO_2 from liquid phase into gas phase, and thus the total gas volume increases (Papale and Polacci 1999; Hill and Prejean 2005; Liu et al. 2005; Wallece 2005; Walter and Amelung 2007). If the magma reservoir is a closed system and is too hard to expand further or to fracture the surroundings, the gas
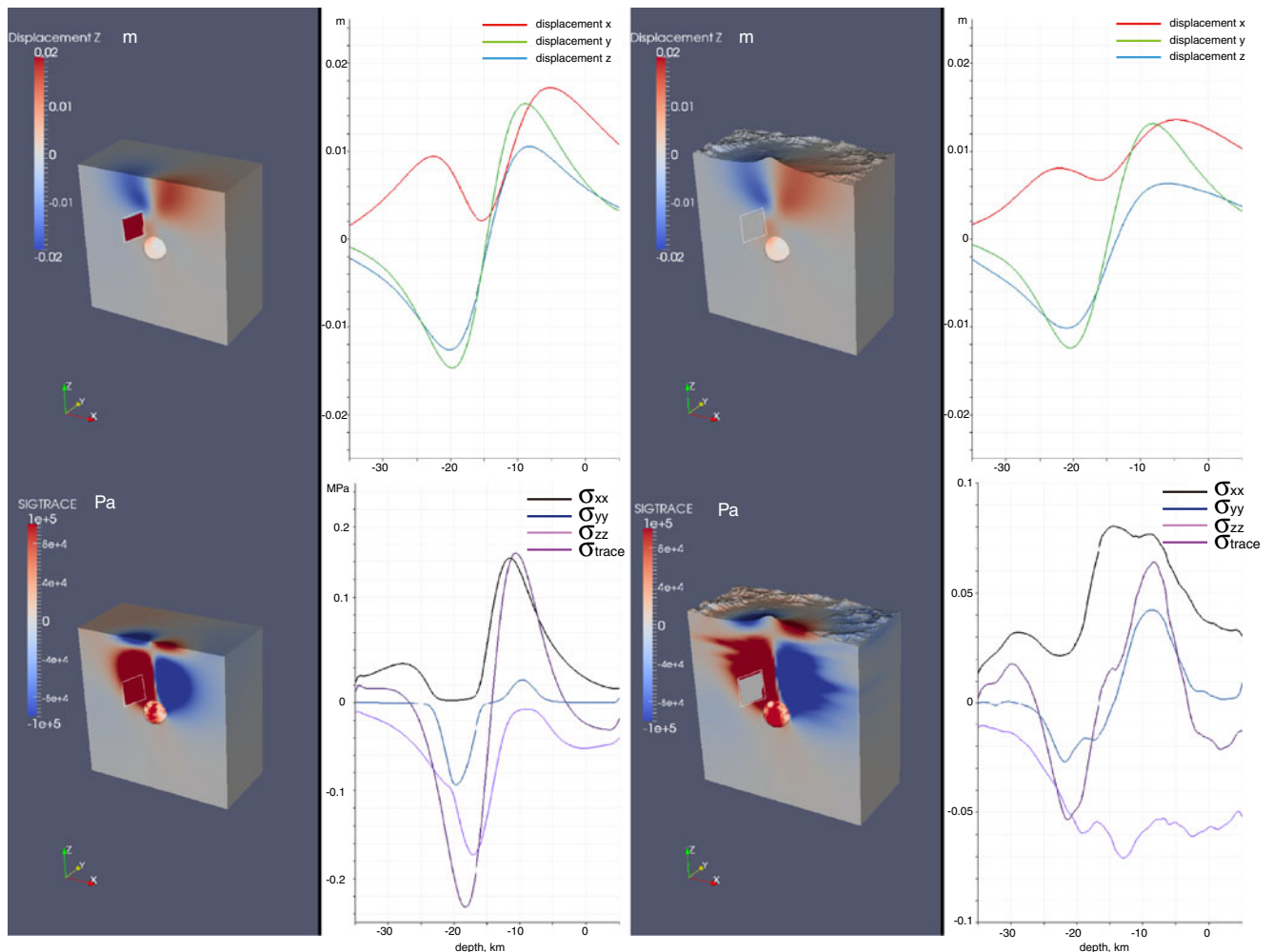

Fig. 9 Sensitivity of FEM numerically simulated crustal deformation on the heterogeneity and topography. The *left plate* illustrates the distribution of displacement and stress for a homogeneous medium with no topography; the *right plates* illustrate that for a heterogeneous medium with topography. In the figure, displacements 0, 1, and 2 correspond to the EW, NS, and UD components, and σ_{trace} is equal to the sum of σ_{xx}, σ_{yy}, and σ_{zz}

component changes back into liquid phase again due to the increase of pressure, that is, this will be a negative feedback cycle. In contrast, if the magma plumbing system is open or has weak walls that are easily expanded or fractured, the increased pressure makes paths for the magma to migrate, and thus the pressure of the magma will be further reduced, and bubbling is accelerated. This is a positive feedback process. The second process involves the stress change in the surrounding rocks. Cracks and/or faults close to the magma system would be unstable due to stress perturbation; this is easy to occur when σ_{dif} is large. These failures can become paths through which magma flows up to trigger an eruption. The lag times between earthquakes and volcanic eruptions may reflect the delays due to these successive processes.

The static stress change caused by the East Shizuoka earthquake was on the order of 0.1–1 MPa at the boundary of magma reservoir, and this is sufficient to trigger earthquakes (Walter et al. 2007, 2009). The lithostatic pressure at the depth of 15 km is about 367.5 MPa; therefore, the perturbation of 1 MPa is only about 0.2 %. So the more

important point is whether the magma has enough potential to erupt or not. We have not yet confident measures to evaluate the eruptive potential of subsurface magma, but the activity of DLP events and some ground deformation are the key observations. A scenario to trigger an eruption is possible when the magma is ready to erupt. The stress change at the boundary may trigger brittle failures, creating paths through which magma can rise, and if the magma gets enough buoyancy to arrive at the ground surface, an eruption will occur. The static stress change of the main Tohoku earthquake is estimated to have been on the order of 0.001–0.01 MPa. This is less than the magnitude required to break new faults but could trigger some perturbation in unstable faults or in the hydrothermal and magmatic systems.

It is considered that a DLP event suggests the subsurface migration of magma, and thus is an important signal for capturing abnormal volcanic activity. As mentioned previously, no eruptions of Mount Fuji have occurred since 1707; however, subsurface magmatic activity has been indicated by DLP events (Ukawa 2005). Figure 7 presents the seismic activity around Mount Fuji from 1996 to 2011. In 2000 and

Fig. 10 Differential stress σ_{dif} distributions for two cases of magma reservoir depths of **a** 15 km and **b** 20 km. The *dashed red circles* indicate the boundary of spherical magma reservoirs. The profile of stress components along the vertical axis is also shown, suggesting the maximum σ_{dif} is at above the magma reservoir
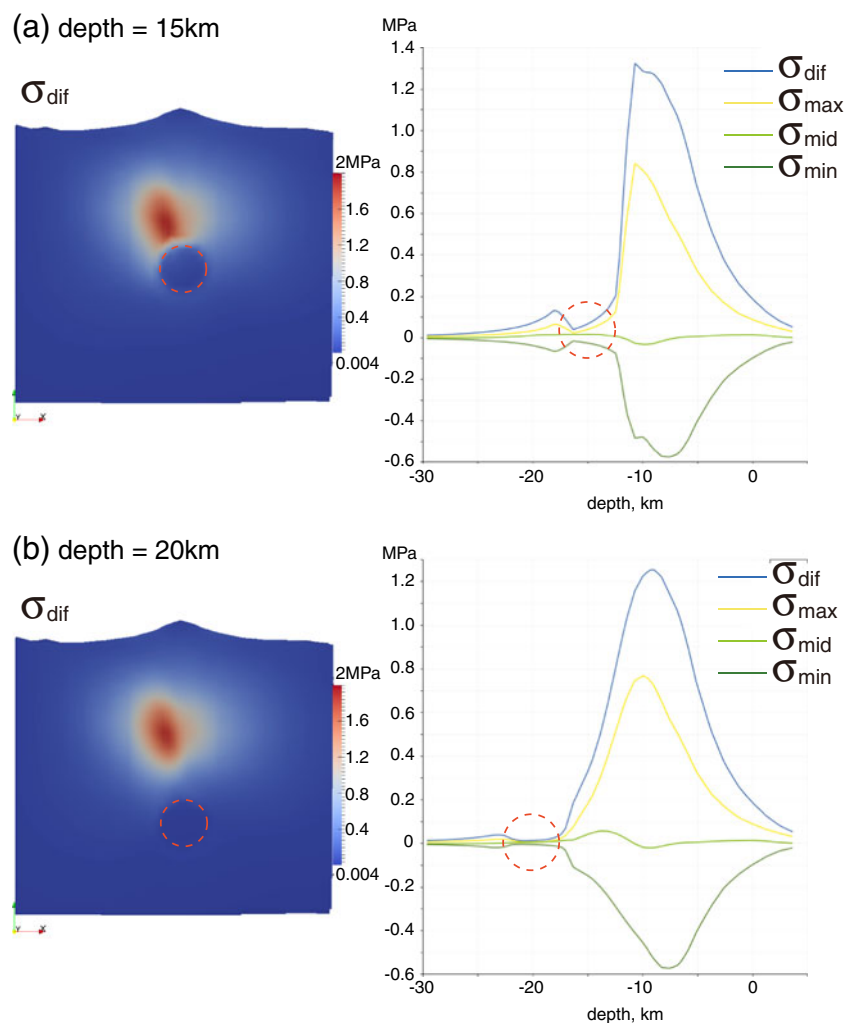
2001, Mount Fuji experienced enormous DLP swarms. They began in August 2000, 2 months after the Miyakejima volcano eruption and consisted of five M_w 6 earthquakes, 36 M_w 5, and 550 M_w 4 earthquakes in 2 months, 160 km south of Mount Fuji. Nishimura et al. (2001) obtained seismic and aseismic sources of this crustal deformation caused by magma migration in the northern Izu Islands. Based on their parameters, we calculated disturbances of the Mount Fuji magma system by FEM (Fig. 8). The estimated stress change is on the order of 10^{-4}MPa, which is only 0.01 of that due to the East Shizuoka earthquake, and this stress change is considered to be too small to trigger an eruption.

Here, it is again noted that, in total, 400 DLP events occurred in 2000 and 2001, and that this is more than the number that occurred during the 20 years from 1980 to 1999. The coupling between the Mount Fuji magmatic system and the PHS is important in analyzing the magmatism of Mount Fuji. Melt generation is linked with the subduction of PHS in view of water supply rate (Turner et al. 2000). This is originated in fluid release from subducting oceanic crust into mantle wedge, as well as the remelting of subducted

sediments toward subduction zones. But this time range is from hundreds kyr (thousand years) to myr (million years), so we infer that the stress change caused by the perturbation of PHS subduction disturbs the pre-existing magma located from upper boundary of PHS toward Moho discontinuity beneath Mount Fuji. The increase of DLP events in 2000 and 2001 may reflect this perturbation. However, in 2011, the disturbances caused by the Tohoku and the East Shizuoka earthquakes were not directly related to PHS subduction or DLP events. The DLP seismicity shows no significant differences bounding Tohoku and East Shizuoka earthquakes, regardless of the static stress changes we calculated. Therefore, there is no evidence of reactivation and Mount Fuji is not close to being ready to erupt at this moment.

Conclusions

The Tohoku megathrust earthquake and its triggered M_w 5.9 East Shizuoka earthquake beneath Mount Fuji imposed significant perturbations on the magma plumbing system.
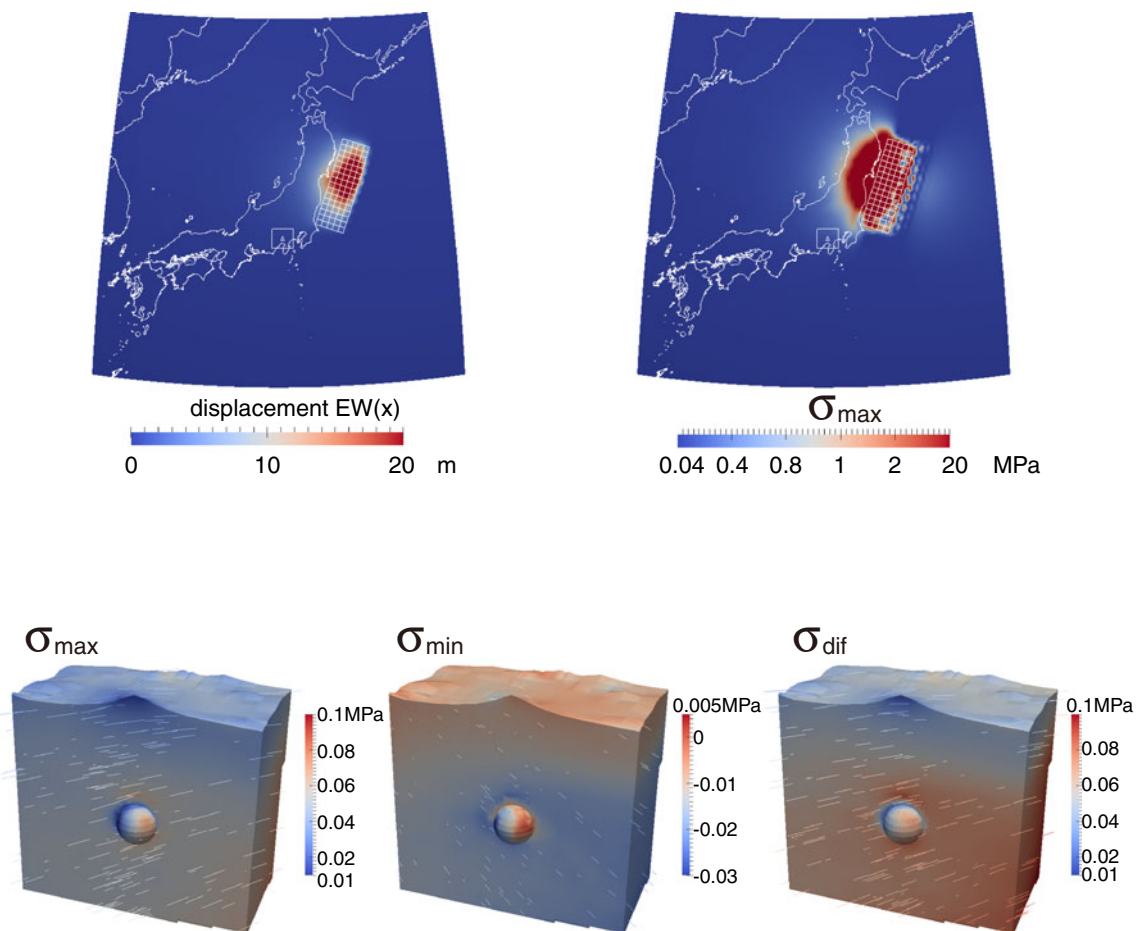

Fig. 11 Disturbance by Tohoku earthquake calculated by the fault model of Koketsu et al. (2011), obtained by joint inversion of teleseismic, strong motion, geodetic and Tsunami data. The fault plane is divided into 80 segments with individual displacement. The disturbance around Mount Fuji is not significantly different from those by the fault model of Ozawa et al. (2011) in Figs. 3 and 4

The deformation of the magma system is calculated based on finite-element modeling of the Japanese mainland and the Mount Fuji region based on the seismic tomography and fault parameters of the Tohoku and East Shizuoka earthquakes. The stress changes at the magma reservoir were extensive: on the order of 0.001–0.01 MPa for the Tohoku earthquake and of 0.1–1 MPa for the East Shizuoka earthquake. These static stress changes are sufficient to promote new fractures at the wall of magma reservoir and magma injection, however, the magma beneath Mount Fuji does not seem to have enough potential to erupt at this moment.

Appendix: sensitivity of simulation results

Our numerical simulation using FEM depends on the assumptions underlying the model. In our analysis, we use seismic fault parameters derived from the inversion of the observation data and the physical properties of the crust and magma are based on the results of seismic tomography. This appendix briefly discusses the sensitivity of our numerical simulation results with respect to three points: (1) the heterogeneity and topography of the crust, (2) the depth of magma reservoir, and (3) the fault model of Tohoku earthquake.

The heterogeneity and topography of the crust

Figure 9 presents examples of simulations of crustal deformation for a homogeneous medium with a no-topography model and for a heterogeneous medium with a topography model. The displacements and stress (in the figure we depict the trace of the stress tensor) suggest different profiles. For example, the peak of EW(x) displacement in the homogeneous-no-topography model is about 0.018 m, whereas that in the heterogeneous topography model is about 0.014 m. The estimated stress changes are on the same order, but the stress trace in the homogenous model has a peak of 0.16 MPa, while that in the heterogeneous model is about 0.06 MPa, less than half of the former case. Therefore, it is better to include the heterogeneity and the actual topography, though we can discuss the order of the stress changes in spite of the ambiguity of the crustal structure.

The depth of magma reservoir

The magma plumbing system beneath Mount Fuji is not clear but we assume it from hypocenter distribution and seismic tomography results. One of the most important factors is the depth of the magma reservoir, so we evaluate how the stress field depends on it. Figure 10 shows the EW cross section of σ_{dif} distribution by East Shizuoka earthquake beneath the summit (left) and the vertical distribution of stress components passing the center of magma reservoir (right). We assume two depths of magma reservoir as (a) 15 km and (b) 20 km. The red dashed circles correspond to the boundary of magma reservoir and it is noted that the σ_{dif} takes the maximum above the reservoir about (a) 1.35 MPa and (b) 1.28 MPa, respectively. Thus, the stress given to the magma system is effective to its depth.

The fault model of Tohoku megathrust earthquake

For the evaluation of stress field change due to Tohoku earthquake, we applied the fault model by Ozawa et al. (2011), which is inverted by the GPS data and the displacements are constant on each of two major faults. Recent analysis by Simons et al. (2011) suggests detail slip distributions on the fault. Similarly, Koketsu et al. (2011) reported a fault model obtained by joint inversion of teleseismic, strong motion, geodetic and Tsunami data. In their model, the fault region is divided into 80 segments with individual displacement. As in Fig. 11, the Tohoku area has different displacement and stress distributions from those obtained as in Fig. 4 by Ozawa et al. (2011), but the stress distribution around Mount Fuji region has no significant difference, comparing Fig. 11 bottom with Fig. 5 top, since Mount Fuji is distant enough from Tohoku region.

References

Asano Y, Saito T, Ito Y, Shiomi K, Hirose H, Matsumoto T, Aoi S, Hori S, Sekiguchi S (2011) Spatial distribution and focal mechanisms of aftershocks of the 2011 off the pacific coast of Tohoku earthquake. Earth planets and space, special issue: first results of the 2011 off the Pacific Coast of Tohoku earthquake

Bautisa BC, Leonila PB, Stein RS, Barcelona ES, Punongbayan RS, Laguerta EP, Rasdas AR, Ambubuyog G, Amin EQ (1996) Relationship of regional and local structures to Mount Pinatubo activity. In: Newhall C, Punongbayan RS (eds) Fire and Mud. University of Washington Press, Seattle, pp 351–370

Birch (1961) The velocity of compressional waves in rocks to 10 kilobars (part II). J Geophys Res 65:1083–1102

Han HD, Wu XN (1985) Approximation of infinite boundary condition and its application to finite element methods. J Comput Math 3:178–192

Hill DP, Prejean S (2005) Magmatic unrest beneath Mammoth Mountain, California. J Volcanol Geotherm Res 146:257–283

Hill DP, Reasenberg PA, Michael A, Arabaz W, Beroza GC (1993) Seismicity in the western United States remotely triggered by the M 7.4 Landers, California, earthquake of June 28, 1992. Science 260:1617–1623

Hill DP, Pollitz F, Newhall C (2002) Earthquake–volcano interactions. Phys Today 55(11):41–47

Japan Meteorological Agency (2011) List of activated volcanoes after 2011 Tohoku earthquake. http://www.seisvol.kishou.go.jp/tokyo/STOCK/kaisetsu/CCPVE/shiryo/122/20110311earthquake.pdf (in Japanese)

Kikuchi A, Dong Q (2011) Earthquake fault analysis by finite element method. Adv Simul 4:100–113

Koketsu K, Yokota Y, Nishimura N, Yagi Y, Miyazaki S, Satake K, Fujii Y, Miyake H, Sakai S, Yamanaka Y, Okada T (2011) A unified source model for the 2011 Tohoku earthquake. Earth Planet Sci Lett 310:480–487

Koyama M (2002) Mechanical coupling between volcanic unrests and large earthquakes: a review of examples and mechanics. J Geogr 111:222–232, in Japanese with English abstract

Koyama M (2007) Database of eruptions and other activities of Fuji Volcano, Japan, based on historical records since AD 781. Yamanashi Institute of Environmental Sciences, Fuji Volano, pp 119–136, in Japanese with English abstract

Lara LE, Naranjo JA, Moreno H (2004) Rhyodacitic fissure eruption in Southern Andes (Cordon Caulle: 40.5 S) after the 1960 (M_w: 0.5) Chilean earthquake: a structural interpretation. J Volcanol Geotherm Res 138:127–138

Linde AT, Sacks IS (1998) Triggering of volcanic eruptions. Nature 395:888–890

Linde AT, Sacks IS, Johnston MJS, Hill DP, Bilham RG (1994) Increased pressure from rising bubbles as a mechanism for remotely triggered seismicity. Nature 371:408–410

Liu Y, Zhang Y, Behrens H (2005) Solubility of H_2O in rhyolitic melts at low pressure and a new empirical model for mixed H_2O–CO_2 solubility in rhyolitic melts. J Volcanol Geotherm Res 143:219–235

Manga M, Broadsky EE (2006) Seismic triggering of eruptions in the far field: volcanoes and geysers. Annu Rev Earth Planet Sci 34:263–291

Marzocchi W, Scandone R, Mulargia F (1993) The tectonic setting of Mt Vesuvius and the correlation between its eruptions and the earthquakes of the southern Apennines. J Volcanol Geotherm Res 58:27–41

Marzocchi W, Selva J, Piersanti A, Boschi E (2003) On the long-term interaction among earthquakes: some insight from a model simulation. J Geophys Res 108. doi:10.1029/2003JB002390

Matsubara M, Obara K, Kasahara K (2008) Three-dimensional P- and S-wave velocity structures beneath the Japan Islands obtained by high-density seismic stations by seismic tomography. Tectonophysics 454:86–103

Mellors R, Kilb D, Aliyev A, Gasanov A, Yetirmishli G (2007) Correlations between earthquakes and large mud volcano eruptions. J Geophys Res 112. doi:10.1029/2006JB004489

Nakamichi H, Watanabe H, Ohminato T (2007) Three-dimensional velocity structure of Mount Fuji and the South Fossa Magna, central Japan. J Geophys Res 112. doi:10.1029/2005JB004161

Nakamura K (1977) Volcanoes as possible indicators of tectonic stress orientation—principle and proposal. J Volcanol Geotherm Res 2:1–16

Navon O, Lyakhovsky V (1998) Vesiculation processes in silicic magmas. In: Gilbert JS, Sparks RSJ (ed) The physics of explosive eruptions. Geol Soc Spec Publ 145: 27–50

Nishimura T, Ozawa S, Murakami M, Sagiya T, Tada T, Kaidzu M, Ukawa M (2001) Crustal deformation caused by magma migration in the northern Izu Islands, Japan. Geophys Res Lett 28:3745–3748

Nishimura T, Sagiya T, Stein RS (2007) Crustal block kinematics and seismic potential of the northernmost Philippine Sea plate and Izu microplate, central Japan, inferred from GPS and leveling data. J Geophys R 112:B0541. doi:10.1029/2005JB004102

Nostro C, Stein RS, Cocco M, Belardinelli ME, Marzocchi W (1998) Two-way coupling between Vesuvius eruptions and southern Apennine earthquakes, Italy, by elastic stress transfer. J Geophys Res 103:24487–24504

Ozawa S, Nishimura T, Suito H, Kobayashi T, Tobita M, Imakiire T (2011) Coseismic and postseismic slip of the 2011 magnitude-9 Tohoku-Oki earthquake. Nature 475:373–377

Papale P, Polacci M (1999) Role of carbon dioxide in the dynamics of magma ascent in explosive eruptions. Bull Volcanol 60:583–594

Simons M, Minson SE, Sladen A, Orgega F, Jiang J, Owen SE, Meng L, Ampuero JP, Wei S, Chu R, Helmberger DV, Kanamori H, Hetland E, Moore AW, Webb FH (2011) The 2011 magnitude 9.0 Tohoku-Oki earthquake: Mosaicking the Megathrust from seconds to centuries. Science 332:1421–1425

Sumita I, Manga M (2008) Suspension rheology under oscillatory shear and its geophysical implications. Earth Plane Sci Lett 269:468–477

Toda N (2011) Mesh generation for the ground model including fault planes. Adv Simul 4:114–121

Toda S, Lin J, Stein RS (2011) Using the 2011 M_w 9.0 off the pacific coast of Tohoku earthquake to test the coulomb stress triggering hypothesis and to calculate faults brought closer to failure. Earth Planets Space 63:725–730

Turner SP, George RMM, Evans PJ, Hawkesworth CJ, Zellmer GF (2000) Time-scales of magma formation, ascent and storage beneath subduction-zone volcanoes. Phil Trans R Soc Lond A 358:1443–1464

Ueda H, Fujita E, Ukawa M, Yamamoto E, Irawan M, Kimata F (2005) Magma intrusion and discharge process at the initial stage of the 2000 activity of Miyakejima, Central Japan, inferred from tilt and GPS data. Geophys J Int 161:891–906

Ukawa M (2005) Deep low-frequency earthquake swarm in the mid crust beneath Mount Fuji (Japan) in 2000 and 2001. Bull Volcanol 68:47–56

Wallece PJ (2005) Volatiles in subduction zone mgmas: concentrations and fluxes based on melt inclusion and volcanic gas data. J Volcanol Geotherm Res 140:217–240

Walter TR (2007) How a tectonic earthquake may wake up volcanoes: stress transfer during the 1996 earthquake–eruption sequence at the Karymsky Volcanic Group, Kamchatka. Earth Plane Sci Lett 264:347–359

Walter TR, Amelung F (2007) Volcanic eruptions following M>=9 megathrust earthquakes: implications for the Sumatra-Andaman volcanoes. Geology 35:539–542

Walter TR, Wang R, Zimmer M, Grosser H, Luhr B, Ratdomopurubo A (2007) Volcanic activity influenced by tectonic earthquake: static and dynamic stress triggering at Mt. Merapi. Geophys Res Lett 34:L05304. doi:10.1029/2006GL028710

Walter TR, Wang R, Acocella V, Neri M, Grosser H, Zschau J (2009) Simultaneous magma and gas eruptions at three volcanoes in southern Italy: an earthquake trigger? Geology 37:251–254

Wolf JP, Song C (1996) Finite-element modeling of unbounded media. Eleventh World Conference on earthquake engineering. Paper no. 70